University of
Reading

Modelling hydrological impacts of agricultural expansion in two macro-catchments in Southern Amazonia, Brazil

Article

Accepted Version

It is advisable to refer to the publisher's version if you intend to cite from the work.

To link to this article DOI: http://dx.doi.org/10.1007/s10113-016-1015-2

Publisher: Springer Berlin Heidelberg

www.reading.ac.uk/centaur

1   Modelling hydrological impacts of agricultural expansion in two macro-catchments in
2   Southern Amazonia, Brazil
3
4   Dr. Gabriele Lamparter[1], glampar@gwdg.de
5   Rodolfo Luiz Bezerra Nobrega[1], rnobreg@gwdg.de
6   Kristof Kovacs[1], kkovacsgwdg.de
7   Dr. Ricardo Santos Amorim[2], rsamorim@ufmt.br
8   Prof. em. Gerhard Gerold[1], ggerold@gwdg.de
9
10   [1] Department of Physical Geography, University of Göttingen, Germany
11   [2] FAMEVZ (Faculdade de Agronomia e Medicina Veterinária), UFMT, Cuiabá, Brazil
12
13   Gabriele Lamparter
14   Institute of Geography,
15   Department of Physical Geography
16   University of Göttingen
17   Goldschmidtstr.5
18   37077 Göttingen
19   0049-551-308026
20   glampar@gwdg.de

21   Abstract:

22   This study presents the setup, calibration, validation and scenario application of the Soil and Water
23   Assessment Tool (SWAT) for two contrasting macro-catchments along the Amazon agricultural
24   frontier in the federal states of Pará and Mato Grosso, Brazil. Calibration and validation of the model
25   is realised for the periods of the most intensive deforestation and agricultural expansion. In order to
26   give consideration to the rapid, however gradual nature of land use change, the model implements
27   an annual land use update combined with a land use dependent soil parameterization of the upper
28   most soil layer. The comparison of these results with the results of a setup with a steady land use
29   distribution shows distinct improvements of the prediction quality. Discharge prediction improves
30   through the application of gradual land use change in the model by 12% for a 1.8% deforestation rate
31   per year and 1.2% for a deforestation rate of 0.7% per year. Consequently, the validated models are
32   applied to four land use scenarios for the period 2026 to 2035. Scenario simulation results show
33   effects on the water balance proportional to land use change. Further, the changes in the water
34   balance follow clear seasonal patterns with highest hydrological effects due to land use change
35   during the rainy season in both catchments. Overall, with continuous deforestation peak discharge
36   increases. Further, the conversion of native to pasture has the highest impact on the water balance.
37   For example, monthly discharge in the rainy season increases by up to 24% for a 13% conversion of
38   Cerrado savannah into pasture.

39

40   Keywords: hydrological catchment model, SWAT, water balance components, land use change, land
41   use update, land use and climate scenarios, Amazon agricultural frontier

42   Length: Abstract: 252, Text body: 5628 words, References: 2589 words, TOTAL: 8609

43   Figures: 4, Tables: 3

1. Introduction:

The ever growing global demand for commodities rapidly pushes the agricultural frontiers around the world further into pristine nature and causes intensification on already existing farmland (Lambin *et al.*, 2001). This is connected to changes in the hydrological balance. For example many studies find that deforestation leads to an increase in discharge (Q, D'Almeida *et al.*, 2007; Davidson *et al.*, 2012), higher floods and more severe water scarcity (Bruijnzeel, 2004; D'Almeida *et al.*, 2007; Fearnside, 2007; Rodrigues *et al.*, 2009). Also other effects, such as changes in the seasonality and the reduction of storage capacity, are frequently reported (Bosch and Hewlett 1982). These changes are further alarming due to their potential to fuel problems connected to the effects of Climate Change (CC, Davidson *et al.*, 2012; Miles *et al.*, 2006). Still, responses to Land Use Change (LUC) are highly variable and depend on the spatial heterogeneity of land use and soil characteristics (Almeida et al. 2006 and 2007). Therefore, it is not surprising that effects of current and future LUC on the hydrological balance, especially of macro-catchments, often remain poorly understood (Bruijnzeel, 2004; Coe *et al.*, 2009; De Roo *et al.*, 2001; DeFries and Eshleman, 2004; Price, 2011).

The largest agricultural frontier with historic and current rapid LUC is located in Southern Amazonia in Brazil (Arima *et al.*, 2011; Fearnside, 2005, 2007). Figure 1 shows the natural vegetation of Brazil, the national highway BR-163 and the Amazon agricultural frontier. Due to its favorable climate for rainfed agriculture, Cerrado - the Brazilian savannah - is under extreme pressure from LUC (Beuchle *et al.*, 2015; Miles *et al.*, 2006). Historically, the deforestation of Cerrado vegetation was the most important source of new farmland in Brazil. Now, the Amazon agricultural frontier expands further towards the North through deforestation of rainforest (Arima *et al.*, 2011), a process boosted by the accessibility through new roads (Wertz-Kanounnikoff, 2005). The ongoing paving of the BR-163 in Central Brazil lead to these typical frontier colonisation processes since the 1990s (Fearnside, 2005).

Only a few macro-catchment studies in the Cerrado biome evaluate the hydrological effects of this comprehensive LUC. However, these studies consistently show a rising trend in Q with deforestation. For example, Costa et al. (2003) showed an increase of Q for the Tocantins River (of which the das Mortes River is a tributary) and an analysis of decadal runoff by Guzha *et al.* (2013b) showed a rise in runoff between 1968 and 1987 for the das Mortes River at Toriquejé (which coincides with 40% Cerrado removal). Macro-catchment LUC research in the rainforest biome is more common. However, these studies show contradictory results regarding hydrological effects (Coe *et al.*, 2009; Lima *et al.*, 2013).

Hydrological models aid the understanding and enable the prediction of changes in the water balance components (WBC) due to future development. However, a reliable prediction of hydrological responses depends on an accurate formal model description of the relevant processes (Beven, 2010), e.g. processes connected to LUC. Typically, the long-term effects of LUC on hydrology are investigated with models calibrated with a steady land use distribution, which is subsequently applied to scenarios with a different and again steady land use distribution (Coe *et al.*, 2009). Here, parameters connected to the different vegetation or land use types of the calibration and scenario periods are determined prior to the model application. This means that hydrological effects of LUC are present in these parameters. Hence, the effects of LUC in a scenario application is predetermined and not tested with observed effects of LUC on hydrology. In this study, we allow the model to adapt land use related parameters to observed hydrological LUC effects by including the gradual nature of LUC in the calibration procedure. The SWAT model is an eco-hydrological model (here version SWAT2012, for documentation see Arnold *et al.*, 2012; Gassman *et al.*, 2007) which includes the possibility of gradual temporal changes on a daily basis (Pai and Saraswat, 2011). Only a few studies

89   have implemented gradual land use change in their SWAT models (Chiang *et al.*, 2010; George, 2014;
90   Guse *et al.*, 2015; Koch *et al.*, 2012; Mani *et al.*, 2014; Wagner *et al.*, 2016). Even fewer have included
91   an evaluation of the performance of the included gradual LUC in the calibration and validation period
92   (Guse *et al.*, 2015; Koch *et al.*, 2012).

93   Aims and objective:

94   Therefore, we present here a study simulating the hydrological effects during the rapid historic LUC
95   in the calibration and validation period for two contrasting macro-catchments: the das Mortes
96   catchment with 17,556 km^2 in the Cerrado biome (-15.14°,-54.16°) and the Jamanxim catchment with
97   37,403 km^2 in the Amazon rainforest biome (-7.34°,-55.84°) including the gradual nature of LUC into
98   the model setup. Furthermore, we assess in how far the inclusion of gradual LUC improves the model
99   prediction by comparing the gradual LUC model setup to a setup with steady land use distribution.
100   Lastly, the calibrated model for both catchments is put into practice for scenarios of future LUC with
101   identical climate scenarios for the period 2026 to 2035 to estimate the magnitude of hydrological
102   changes dependent on potential future LUC.

103   2.   Study area and period:

104   The two catchments were chosen in areas of rapid historic deforestation and dominant rainfed
105   agriculture to ensure that LUC effects are not influenced by technical water management (e.g. dams
106   and irrigation). The das Mortes catchment is situated in the federal state of Mato Grosso. It is located
107   on top of a plateau of cretaceous sandstone maintaining a large deep aquifer (Schneider, 1963). The
108   climate is tropical wet and dry (dry period: May to September, Climate-Data.org, 2015), with an
109   precipitation (P) of 1784 mm a^{-1} (Primavera do Leste , Global Weather Data, 2015). The dominant soil
110   types are the highly permeable Ferralsol (70%) and Arenosol (23%, see the Brazilian Agricultural
111   Research Corporation (EMPRAPA) soil map profiles, ESALQ, 2015). The average slope is 2.9%. Mato
112   Grosso is the Brazilian state with the highest deforestation rate (Macedo *et al.*, 2012). Deforestation
113   rates are declining since 2000 (Davidson *et al.* 2012) due to exhaustion of forested areas on arable
114   soils which are not protected in reservations. Parallel to the slowing deforestation in the last 15-20
115   years, land use in Mato Grosso and especially in the das Mortes catchment is characterised by
116   intensification with a shift towards double cropping and minimum tillage (Beuchle *et al.*, 2015;
117   Galford *et al.*, 2010; Hunke *et al.*, 2015b). For the das Mortes catchment, the historic land use
118   classification was relalised with Landsat satellite imagery analysis by Schlicht (2013) with an accuracy
119   of 97% and an omission error of less than 1% (for 1988 and 1998). Deforestation for 1970 prior to be
120   the first Landsat image was 1% (IBGE, 2015). Consequently, the mid-1970s to mid-1980s are
121   identified as the period with the most intensive deforestation in this area (Table 1). This coincides
122   with the period 1968-1987 for which Guzha *et al.* (2013b) showed an increase in Q despite steady P
123   records. For the das Mortes catchment, satellite and statistical information is not sufficient to reliably
124   distinguish between cropland and pasture land uses. Consequently, the land use category "Non-
125   Forest" was defined.

126   The Jamanxim catchment is located in the central southern part of the Amazon rainforest in the state
127   of Pará. Its geological structure consists of Ordovician sedimentary and Precambrian metamorphic
128   rocks (usouthal.edu, 2016). It has a tropical monsoon climate and a dry period from June to August
129   (Climate-Data.org, 2015) with an annual P of 2232 mm (Novo Progresso, Global Weather Data, 2015).
130   The dominant soil type is the deeply weathered Acrisol (84%, see ZEE, 2015). The average slope is
131   12.7%. The historic land use classification was realised with Landsat satellite imagery by Macioscheck
132   (2013, for 1998, 2007 and 2011) with an accuracy of 99% (Maciocheck, 2013). Deforestation rates
133   peaked in the 2000s to open up pastures for cattle grazing. Compared to the total Brazilian Amazon

134   Basin, pre 1990 deforestation in the Jamanxim catchment was comparatively low, increasing rapidly
135   in the 1990s and 2000s, now reaching 15% (see Tabel 1).

136   For the das Mortes catchment, the period from 1977 to 1981 was chosen for calibration and 1982 to
137   1986 for validation. This period combines good Q and P records, the most rapid LUC and a change in
138   the relationship of Q and P. In the Jamanxim catchment the most rapid deforestation occurred in the
139   last decade. Further, a longer time series of Q is only available from 2000 to 2009. Consequently, this
140   period was chosen, with 2000 to 2004 for calibration and 2005 to 2009 for validation.

141   Furthermore, the scenario application in both catchments was set to the decade around the year
142   2030. Future LUC in the region is mainly dependent on political, economic and social development.
143   The LANDSHIFT model (Schaldach *et al.*, 2011; Schaldach and Koch, 2009) has the capability to
144   estimate future LUC along storylines sketching political, economic and social development. For the
145   two study regions, four different scenarios developed in an interdisciplinary effort by the Carbiocial
146   project (carbiocial.de, Schönenberg *et al.*, this issue) are taken into account: A *trend* scenario, where
147   the development seen in the last decade will continue into the future, a *sustainable* scenario where
148   regulations favour sectors with the most efficient land use, i.e. reduction of cattle ranching and a
149   focus on crop production. Further, both the *legal* and *illegal* scenarios suggest a rapid agriculture
150   expansion, either *legal* with the perpetuation of current protective areas or *illegal* without (for a
151   detailed description refer to Göpel and Schaldach, this issue). The fractions of the land use in 2020,
152   2025 and 2030 of the four LANDSHIFT calculated scenarios are also listed in Table 1. The land use
153   distribution in the das Mortes catchment does not ideally reflect the overall development associated
154   with the scenarios. For example, the *illegal* scenario displays the highest fraction of scrubland
155   vegetation (Cerrado). The *trend* scenario is marked with a 12-14% higher fraction of pasture. The
156   highest fraction of cropland is associated with the *sustainable* scenario and continuously declines
157   from *legal* to *illegal* to *trend* scenario. For the Jamanxim catchment, the scenario differences are as
158   intended with the highest remaining forest cover and a complete elimination of pasture for the
159   *sustainable* scenario. In 2030, the *legal* and *illegal* scenarios show a land use with 23% more forest
160   clearance in 2030 compared to the *sustainable* scenario. However, they display different
161   deforestation rates in the years before where the *legal* scenario behaves similar to the *sustainable*.
162   Furthermore, deforestation is distributed differently over the catchment. The *trend* scenario has an
163   intermediate fraction of forest removal and an intermediate extend of pasture.
164
165   3.   Setup and parametrisation of the SWAT2012 model
166   a.   Topography:
167   The SWAT model depends on a distributed representation of the catchment geometry and its river
168   network (here, ASTER data sets (version 2) with 30 m grid cell resolution). It was delineated for the
169   catchment outlet points at Toriquejé in the das Mortes catchment (-15.25°, -53.06°) and at Jardim do
170   Ouro in the Jamanxim catchment (-5.50°, -55.83°). For the das Mortes catchment, sub-catchments
171   are as best determined according to municipality borders to utilise information from the Brazilian
172   Institute of Geography and Statistics (IBGE). In the Jamanxim catchment, sub-catchments include
173   areas with similar land use.

174   b.   Hydrological Response Unit (HRU) definition and management operations:
175   For each sub-catchment HRUs with a unique soil, slope and land use are defined. SWAT allows the
176   selective parametrisation of these smallest units of execution. The management in the das Mortes
177   catchment includes double cropping (soy and corn) and cattle grazing for Non-Forest, depending on
178   the soil type (good quality leads to cropping, poor quality to grazing). No management is

179 implemented in Cerrado and gallery forest HRUs. For the Jamanxim catchment only HRUs with
180 pasture are managed with cattle grazing.

c. Vegetation parametrisation

182 Parametrisation of new land use types were added to the SWAT2012 data base using a combination
183 of literature data and own observations. Parameters for Cerrado and gallery forest were extracted
184 from a range of eco-physiological and hydrological studies (Coe *et al.*, 2009; Davidson *et al.*, 2012;
185 Lathuillière *et al.*, 2012; Pongratz *et al.*, 2006). For pasture, the SWAT 2012 database was extended
186 with area specific information (Allen *et al.*, 1998; Barona *et al.*, 2010; Hayhoe *et al.*, 2011; Lathuillière
187 *et al.*, 2012). Also, rainforest was added using literature information (Granier *et al.*, 2000; Hayhoe *et
188 al.*, 2011; Kergoat, 1998; Sellers *et al.*, 1989, 1996). A particular challenge is SWAT's dependency on
189 the dormancy during the winter season for the reinitiation of the growing season for perennial
190 plants. This process is not a valid growing pattern in the tropics. Therefore, the plant growth
191 modification of Strauch and Volk (2013) - originally developed for the Cerrado biome - was applied
192 for Cerrado, rainforest, gallery forest and pasture. Here, the start of the growing season is triggered
193 by an increase of available soil water. Evapotranspiration and leaf area index (LAI) curves were
194 adjusted by manually changing SWAT specific parameters determining the LAI curve shape to match
195 observations (Christoffersen *et al.*, 2014; Giambelluca *et al.*, 2009; Lima *et al.*, 1990; Oliveira, 2014;
196 Oliveira *et al.*, 2014; Strauch and Volk, 2013).

d. Soil parametrisation

198 With regard to soil surface parametrisation, surface runoff (Qsur) and infiltration are determined by
199 the SCS Curve Number (CN) method (Mishra and Singh, 2003). The initial parameter estimates are
200 taken from Drewry *et al.* (2008); Hunke *et al.* (2015b); McGrath *et al.* (2001) and Oliveira *et al.*
201 (2014). Mean values for soil texture and bulk density were determined through statistical analysis of
202 the RADAM soil profile data base (ESALQ, 2015; Jacomine, 2013). Lastly, hydraulic conductivity (k_{sat})
203 for the main soil types was defined according to our own in situ measurements with a Compact
204 Constant Head Permeameter (Amoozegar and Warrick, 1986).

e. Implementation of gradual land use change

206 The LUC for the calibration, validation and each scenario application was calculated separately in
207 each sub-catchment and updated on an annual basis. The land use distribution for years without
208 information was estimated with linear interpolation, also for each sub-catchment separately. On
209 average during the calibration and validation periods, every year 1.8% of Cerrado vegetation was
210 converted into Non-Forest in the das Mortes catchment. In the Jamanxim catchment, 0.7% forest
211 was transformed into pasture. The LUC is concentrated in the Western parts of the catchment, which
212 is crossed by the BR 163. The sub-catchments crossed by the BR 163 have a deforestation rate of
213 2.4% p.a.. However, gradual LUC is connected to some shortcomings, since the SWAT land use
214 update function allows only to redefine the fractions of existing HRUs, not the inclusion of new HRUs.
215 In some cases it was not possible to redefine the land use class without also redefining either slope
216 or soil class. In these cases areas of HRUs under LUC were preferable assigned to HRUs with the most
217 similar soil type and slope class. Typically, for calibration, validation and scenario application this
218 affected areas of less than 2.5%. Only in the case of the calibration and validation period in the Rio
219 das Mortes 6% of the catchment area had to be reassigned from the Latosolo Vermelho-Amarelo to
220 the Latosolo Vermelho soil class. Since this are small areas and in the case of the soil reassignment
221 similar soil types, we do not expect this to causes considerable changes to water balance calculation.

f. Weather data:

223 The daily weather records from INMET and ANA (Instituto Nacional de Meteorologia, BDMEP 2015
224 and Agencia National de Aguas, ANA 2015) are applied in the das Mortes catchment. The P records
225 are cross referenced for validity with CFSR reanalysed forecast data on a 35 km raster resolution
226 (Fuka *et al.*, 2014; Global Weather Data, 2015). For the das Mortes catchment, INMET and CFSR
227 weather data are on average similar. In the Jamanxim catchment, due to the lack of weather data
228 records, CFSR data is used as the source of weather information. Comparing the rainfall data with the
229 closest weather station in Itaituba shows that the CFSR data is overestimating P in the wet season
230 and underestimating P in the dry season. The Itaituba INMET station records an annual average of
231 2070 mm (1530 mm in the rainy season and 540 mm in the dry season) for the period from 1961 to
232 2010, whereas the mean of the CFSR data sets annual P to 2400 mm per annum (2105 mm in the
233 rainy season and 295 mm in the dry season) for 1979 to 2014. From this a P correction factor was
234 calculated for each month of the year which adapts the CFSR data to the level measured at Itaituba.
235 For all LUC scenarios, the IPPC SRES A1B climate scenario downscaled with the STAR method (Böhner
236 *et al.*, 2013; Böhner, this issue) for the period 2026 to 2035 is applied. The scenario predicts a
237 considerable reduction in annual P of 29% in the das Mortes catchment and 32% in the Jamanxim
238 catchment in comparison to the calibration and validation period.

239   g.   Model calibration and validation:
240 The model calibration is based on the optimisation of the modelled monthly Q (Qmod) at the outlets
241 of the catchments towards the observed values (Qobs). The daily Q information ("ANA" 2015, station
242 2650000) was transferred into monthly values. Both the calibration, and the estimation of the
243 predictive uncertainty was automated with the software tool SWAT-CUP (Abbaspour, 2007) with the
244 Sequential Uncertainty Fitting (SUFI-2) method (Abbaspour *et al.*, 2004).
245 The calibration concentrates on two groups of calibration parameters: Firstly, parameters, which are
246 generally sensitive, such as groundwater related parameters. These are adapted in the calibration
247 procedure for the whole catchment. Secondly, parameters connected to land use, which are
248 parameters defining vegetation growth and properties of the upper soil, such as CN and k_{sat}. In the
249 calibration procedure these were adapted for each soil and land use type combination separately.
250 For all calibration parameters, physically meaningful ranges are defined as the parameter space.
251 From these, random samples are taken with the latin hypercube method (Abbaspour, 2007) for each
252 of the 1500 iterations for one calibration run.
253 At the end of the calibration run, the best estimation is identified with the Nash-Sutcliffe Efficiency
254 index (NS) as the objective function. Further, the coefficient of determination (R^2), percentual bias
255 (PBIAS) and Root Mean Error (RME) are also calculated for the identified best estimation.
256 The uncertainty is calculated from the cumulative distribution of the output variable(s) (i_t) for every
257 output time step (t, here monthly). The 95% confidence interval (95CI) is the range between the
258 2.5% and 97.5% levels of the distribution of i_t, which relates to the reliability of the estimation
259 procedure, not the probability of a value being estimated. Further, the p-factor (fractions of values
260 within 95CI) and the r-factor (relative bandwidth of 95CI = $\frac{95CImax-95CImin}{(i_t mean+i_t sd)-(i_t mean-i_t sd)}$) are evaluated.
261 Each calibration run with 1500 iterations suggests a progressingly smaller calibration parameter
262 range until the 95CI of the model output is close to the standard deviation of the measured data. In
263 order to generate comparable conditions for the calibration of the setup with and without gradual
264 land use change, the initially identical parameter space was set to half its range in each consecutive
265 calibration run. For each setup, calibration runs with 1500 iterations are repeated three times to
266 achieve the before mentioned quality criterion. The final calibration parameter range from the setup
267 with gradual land use change is then brought forward to be executed for the validation period (and
268 the steady land use model setup from 1988 for the das Mortes catchment and from 2007 for the

269 Jamanxim catchment). For the scenario application, only the optimum value for each calibration
270 parameter defined through the setup including gradual land use change is implemented. In order to
271 highlight the performance of the land use update setup, the predictive error (PE=Qobs-Qmod) of the
272 catchment discharge is evaluated. Further, the LOcally WEigted Scatterplot Smoothing (LOWESS) as a
273 nonparametric regression using multiple regression models (Cleveland, 1981) is applied to PE to
274 visualise trends concealed by the variability of PE.

275   4. Results
276   a. Optimum values of selected calibration parameters:
277 A calibration parameter with fundamental influence especially on the distribution of water between
278 the rainy and the dry season is the groundwater delay factor (given in days). This is a calibration
279 parameter independent of land use, which determines the baseflow (Qgw) contribution to discharge.
280 Since very little is known about the groundwater dynamics in both catchments, this parameter was
281 defined during the calibration procedure. It displays a clear difference between the two study
282 catchments. In the das Mortes catchment, Qgw makes up for ~80% of Q, fed by an extensive
283 groundwater buffer, represented by an optimum groundwater delay of 316 days, maintaining
284 minimum Q at 25% of the maximum Q. In the Jamanxim catchment, Q generation is foremost
285 influenced by interflow (Qint), causing Q to be maintained at 5 to 10% of the maximum, which is
286 associated with a much shorter groundwater delay of 74 days. This difference can be explained by
287 the following characteristics of the catchments. The das Mortes catchment is dominated by a mostly
288 flat relief (Guzha et $al.$, 2013a) with sandy soils, causing water to percolate freely to the deep aquifer.
289 Further, it is underlain by a pan like geological structure of cretaceous sandstone supporting an
290 aquifer of up to 1300 m depth (Parana Mesozoic and Paleozonic groundwater province, Schneider,
291 1963). The Jamanxim catchment belongs to a greater part to the Central Precambrian groundwater
292 province, which typically only supports a thin deep aquifer and wells with low yields (Schneider,
293 1963). Further, the relief is comparable steep supporting a faster lateral runoff.
294 There is strong evidence that LUC alters particularly the properties of the upper soil layer (Bruijnzeel,
295 2004; Christoffersen et $al.$, 2014). Therefore, CN and k_{sat} of the upper most soil layer, which were
296 initially parameterized according to soil type only, were adapted during the calibration procedure
297 independent for each soil and land use type. Table 2 lists their land use dependent optimum values
298 as suggested by the final iteration of the calibration runs with gradual land use change. Overall CN
299 values are low, confirming the initial high infiltration into the upper soil layer in both catchments due
300 to permeable soils. Nevertheless, the calibration procedure identified lower CN for natural
301 vegetation compared to cropland and pasture. The calibration also suggests higher k_{sat} values for
302 natural vegetation compared to pasture and cropland in both catchments. Such a change of
303 properties in the upper soil layer with LUC is in accordance with own measurements and literature
304 data (Christoffersen et $al.$, 2014; Hunke et $al.$, 2015a).

305   b. Prediction quality:
306 The identified optimum calibration parameters result in a Qmod in good accordance with Qobs.
307 Table 3 shows that if we are looking at NS both the das Mortes and the Jamanxim catchment have a
308 very good to good performance rating for the calibration, validation of both land use update and
309 steady land use application (Moriasi et $al.$, 2007). The values are well within the results reported for
310 other macro-catchment models (Fukunaga et $al.$, 2015; Guzha et $al.$, 2013a; Nandakumar and Mein,
311 1997; Schilling et $al.$, 2008). Divergences between the land use update and steady land use
312 application for the das Mortes catchment are reflected in NS and the r-factor. NS is considerable
313 higher for the calibration with gradual land use. Further, the r-factors of both the calibration and
314 validation period in the das Mortes catchment are smaller than in the steady land use application.

315   Similar differences in the Jamanxim catchment are less pronounced, however perceivable. Here, the
316   small fraction of areas with LUC (see Table 1) compared to the large area of remaining rainforest
317   buffers the responses of the hydrological balance.
318   To highlight the different performance of the land use update and the steady land use setup, Figure
319   2a shows the PE between Qobs and model Qmod for land use update (PE_1) and steady land use (PE_2)
320   setup in the das Mortes catchment. PE shows that both overprediction (negative PE) and
321   underprediction (positive PE) are more pronounced for a steady land use setup (PE_2). LOWESS
322   regressions are applied to show the trend in PE over the application period. Both PEs decline towards
323   the end of the period. Additionally, the difference between PE_1 and PE_2 declines, showing that the
324   steady land use setup prediction becomes more accurate towards the date of the applied land use
325   distribution (from the year 1988). Similar, but less pronounced differences can be seen in the PEs for
326   the Jamanxim catchment in Figure 2b. Again, the steady land use setup has both a higher over- and
327   underprediction of the observed discharge. If looking at the LOWESS regression, in the first seven
328   years of the application period, the land use update setup shows a slightly lower underprediction
329   compared to the steady setup. For the year 2007, the land use update PE_1 and the steady land use
330   PE_2 are the same.

331   c.   Scenario application
332   The four LUC scenario applications in each catchment (for degree of LUC refer to Table 1) were
333   executed with identical climate projections to reflect purely on alteration of WBCs due to LUC. Mean
334   annual WBCs in relation to mean annual P for the scenario period from 2026 to 2035 are shown in
335   Figure 3a and b. In the das Mortes catchment, the WBC in the *sustainable*, *legal* and *illegal* scenarios
336   are of the same magnitude reflecting the distribution of land cover with only a gradual change of
337   Cerrado and cropland. Only the *trend* scenario with the highest fraction of pasture results in a higher
338   Q due to a lower evapotranspiration and k_{sat} reduction. Moreover, it is the scenario with the highest
339   surface runoff, however rates are generally limited to less than 1 mm month^{-1}. Considerable surface
340   runoff (> 10 mm month^{-1}) only occurs in the Western parts of the catchment (on Latosolo) during the
341   very wet month of February in 2034 with more than 400 mm P causing soil saturation and therefore
342   soil saturation excess runoff.
343   The land cover scenarios in the Jamanxim catchment show gradual differences between all scenarios.
344   Differences in Q are mirrored in ET with the lowest Q and highest ET for the *sustainable* scenario with
345   forest protection and an elimination of pastures. Surface runoff is limited to the steep headwater
346   catchments in the south.

347   Additionally to the changes in the overall WBC, the seasonality of runoff generation changes. Figure 4
348   shows monthly ΔQ for the *sustainable*, *legal* and *illegal* scenario, where ΔQ is the difference between
349   Q of the *trend* scenario and Q of each of the other scenarios ($\Delta Q = Q_{trend\ scenario} - Q_{other\ scenraios}$). For the
350   seasonal comparison, the *trend* scenario Q is also plotted. The differences in mean Q are not
351   distributed equally throughout the year but predominantly associated with the peak discharge
352   months. In the das Mortes catchment, highest ΔQ is found during rising Q at the beginning of the
353   rainy season. Additionally, during the low flow period in dry years, the *trend scenario* maintains
354   higher flows. The *trend* scenario has the highest proportion of pasture, which means that pasture
355   generates more runoff at the beginning of the rainy season and higher Qgw compared to the other
356   land use types. This is in accordance with research showing that pasture causes higher peak
357   discharge (Costa *et al.*, 2003; Drewry *et al.*, 2008; Guzha *et al.*, 2013b; Hodnett *et al.*, 1995; Hunke *et*
358   *al.*, 2015a). We account this to the ready available leaf area resulting in immediate
359   evapotranspiration (Cerrado) of the received P and a higher water storage capacity of the less
360   compacted soil.

361   In the Jamanxim catchment, largest ΔQs are associated with the *sustainable* scenarios, with the
362   highest fraction of remaining forest cover. The *trend* scenario has a land cover distribution similar to
363   the *legal* and *illegal* scenario and therefore ΔQs are very low. The pattern of ΔQ for the *sustainable*
364   scenario follows a pattern of lower discharge, especially during the rising stage of the wet season and
365   the maintenance of higher flows during the dry season.

366   This seasonal pattern is potentially characteristic for hydrological effects of LUC in areas with
367   pronounced wet and dry periods, since it was also observed in a similar SWAT model application
368   including gradual LUC by Wagner *et al.* (2016) for a catchment in India with monsoon climate.

369   5.   Discussion:

370   For our catchments with intensive LUC in the calibration and validation period, the model setups
371   including gradual land use change show a better performance than the model setups with a steady
372   land use distribution. This is reflected in the throughout smaller PE of the land use update setup in
373   the two contrasting catchments. The difference between the error calculations of the two setups is
374   dependent on the degree of LUC. In the das Mortes catchment with 1.8% deforestation per annum,
375   absolute PE_1 is on average 19 mm per annum smaller (corresponding to 11.2% Q or 1.8% P) than
376   absolute PE_2. For the Jamanxim catchment with 0.7% deforestation per annum, the difference is 8
377   mm per annum (corresponding to 1.2% Q or 0.4% P).

378   Classically, land use influence on water balance is dependent on differences in evapotranspiration.
379   Here we also included the differentiation of properties of the upper soil layer under different land
380   use. For each land use and soil type combination, these are adapted independently in the calibration
381   procedure. The calibration results support that LUC is accompanied by soil compaction processes
382   through deforestation and agricultural land use. Remarkably, our results fit well with reported field
383   research findings, regarding the soil compaction through land use in this area (Bruijnzeel, 2004;
384   Christoffersen *et al.*, 2014; Drewry *et al.*, 2008; Hunke *et al.*, 2015b; Nobrega *et al.*, 2015; Scheffler *et*
385   *al.*, 2011). These established higher optimum CN and lower optimum k_{sat} values for cropland and
386   pasture compared to natural vegetation have a clear effect on Q prediction. This agreement of field
387   records and calibration outputs indicates an adequate representation of pedo-hydrological processes
388   connected to LUC.

389   The model applications are an advanced tool to contribute to the discussion about changes of WBC
390   due to future LUC, since they include both, the change of evapotranspiration and soil properties with
391   LUC. Moreover, in many cases LUC effects on hydrology are subordinate to CC effect. Therefore, the
392   different LUC scenarios are simulated with the same climate scenario to ensure that all observed
393   hydrological effects are purely LUC effects. According to our results, for both the das Mortes and the
394   Jamanxim catchment, the model shows an increase of Q with continuous deforestation. For the das
395   Mortes catchment, a reduction of Cerrado of 5% and an increase of pasture of 12% (compare *illegal*
396   to *trend* scenario 2030) results in an 3.4% increase of annual Q, which confirms findings of (Costa *et*
397   *al.*, 2003; Guzha *et al.*, 2013a). In the Jamanxim catchment, 24% more deforestation (compare
398   *sustainable* to *illegal* scenario 2030) increases Q by 13 mm per annum (2.0% of Q, 0.8% of the P).
399   However, Coe *et al.* (2009) and Lima *et al.* (2013) stress the fact, that P is dependent on recycled
400   transpiration from the forest vegetation (P-feedback). This process is most effective in the rainforest
401   biome, where studies state that with complete deforestation, P is reduced by 20 to 35% (D'Almeida
402   *et al.*, 2007; De Paiva *et al.*, 2013; Nobre *et al.*, 1991). Coe *et al.* (2009) and Lima *et al.* (2013) both
403   showed with the application of a model with and without P-feedback, that the inclusion of P-
404   feedback is crucial for Q prediction in the Amazon rainforest biome. Our Jamanxim results are similar
405   to the results of the Coe *et al.*, (2009) model without P-feedback, where a deforestation of 26% leads

406 to an 8% increase of Q, however, with P-feedback for the same area Coe *et al.* (2009) find Q to
407 decrease by 12%. Consequently, for our model a more accurate prediction needs to include P-
408 feedback. This cannot be realised in SWAT directly, but needs to be incooperated in the climate
409 model. In the current STAR climate prediction an adaption of P according to the different LUC
410 scenarios is not implemented, not least because of the complex nature of P-feedback, which is highly
411 dependent on deforestation pattern (Negri *et al.*, 2004). However, our future research aims to
412 include these complex feedbacks.

413 Independent of P-feedback effects, a comparison of scenarios suggests a severe influence of
414 conversion into pasture on the WBC. In the das Mortes catchment, a 13% increase of pasture
415 (compare *trend* and *sustainable* scenario) causes a 4 to 27 mm (13.3-73.0%) increase in monthly Q at
416 the beginning of the rainy season (December and January) due to decreased evapotranspiration and
417 an increase in Qsur and interflow (Qint, Fig. 4a). The differences in Q seasonality for increased Q due
418 to pasture and cropland area are similar in the Jamanxim catchment. For example, 14% more
419 cropland (compare *trend* and *legal* scenario in 2030) leads to up to 30 mm month^{-1} higher discharge
420 during the rainy season.

421
422   Conclusions:
423 - Through the implementation of gradual land use change, the accordance of Qmod and
424   Qobs is improved by 11.2% in the catchment with 1.8% annual deforestation and by 1.2%
425   in the catchment with 0.7% annual deforestation. This demonstrates that in regions with
426   intensive LUC during the application of a hydrological model, the inclusion of gradual
427   land use change is necessary to ensure the best possible prediction quality.
428 - The model predictions for four land use scenarios in two fundamentally different macro-
429   catchments show changes in WBC predominantly during the wet season, with strongest
430   effects for the conversion of native vegetation (Cerrado and rainforest) to pasture.
431 - In the das Mortes catchment with the more pronounced dry season, the ground water
432   components are more relevant for annual discharge generation. The more seasonal
433   climate also coincides with more pronounced LUC effects on hydrology at the beginning
434   of the rainy season, whereas under less seasonal rainforest climate (≤ 3 arid month), LUC
435   effects on hydrology are apparent during the whole rainy season.

439   References:

440   Abbaspour KC. 2007. User manual for SWAT-CUP, SWAT calibration and uncertainty analysis
441   programs. *Swiss Federal Institute of Aquatic Science and Technology, Eawag, Duebendorf,*
442   *Switzerland*.

443   Abbaspour KC, Johnson CA, van Genuchten MT. 2004. Estimating uncertain flow and transport
444   parameters using a sequential uncertainty fitting procedure. *Vadose Zone Journal* **3**(4): 1340. DOI:
445   10.2136/vzj2004.1340.

446   Allen RG, Pereira LS, Raes D, Smith M, others. 1998. Crop evapotranspiration-Guidelines for
447   computing crop water requirements-FAO Irrigation and drainage paper 56. *FAO, Rome* **300**(9).

448   Amoozegar A, Warrick AW. 1986. Hydraulic Conductivity of Saturated Soils: Field Methods. *Methods*
449   *of Soil Analysis: Part 1—Physical and Mineralogical Methods* 735–770. DOI:
450   10.2136/sssabookser5.1.2ed.c29.

451   Arima EY, Richards P, Walker R, Caldas MM. 2011. Statistical confirmation of indirect land use change
452   in the Brazilian Amazon. *Environmental Research Letters* **6**(2): 24010. DOI: 10.1088/1748-
453   9326/6/2/024010.

454   Arnold JG, Moriasi DN, Gassman PW, Abbaspour KC, White MJ, Srinivasan R, Santhi C, Harmel RD,
455   Van Griensven A, Van Liew MW, others. 2012. SWAT: Model use, calibration, and validation.
456   *Transactions of the ASABE* **55**(4): 1491–1508.

457   Barona E, Ramankutty N, Hyman G, Coomes OT. 2010. The role of pasture and soybean in
458   deforestation of the Brazilian Amazon. *Environmental Research Letters* **5**(2): 24002.

459   Beuchle R, Grecchi RC, Shimabukuro YE, Seliger R, Eva HD, Sano E, Achard F. 2015. Land cover
460   changes in the Brazilian Cerrado and Caatinga biomes from 1990 to 2010 based on a systematic
461   remote sensing sampling approach. *Applied Geography* **58**: 116–127. DOI:
462   10.1016/j.apgeog.2015.01.017.

463   Beven K. 2010. *Environmental modelling: an uncertain future?* CRC Press: Routledge.

464   Böhner J. this issue. Paradigm in modelling climate change – results with STAR and WRF. .

465   Böhner J, Dietrich H, Fraedrich K, Kawohl T, Kilian M, Lucarini V, Lunkeit F. 2013. Development and
466   implementation of a hierarchical model chain for modelling regional climate variability and climate
467   change over southern Amazonia. *Interdisciplinary Analysis and Modeling of Carbon-Optimized Land*
468   *Management Strategies for Southern Amazonia, Universitätsdrucke Göttingen* 119–128.

469   Bozana Maciocheck. 2013. Change Detection im Wassereinzugsgebiet Novo Progresso (Pará,
470   Brasilien). Göttingen, Germany.

471   Bronstert A, Niehoff D, Bürger G. 2002. Effects of climate and land-use change on storm runoff
472   generation: present knowledge and modelling capabilities. *Hydrological Processes* **16**(2): 509–529.
473   DOI: 10.1002/hyp.326.

474   Bruijnzeel LA. 2004. Hydrological functions of tropical forests: not seeing the soil for the trees?
475   *Agriculture, Ecosystems & Environment* **104**(1): 185–228. DOI: 10.1016/j.agee.2004.01.015.

476 Chiang L, Chaubey I, Gitau MW, Arnold JG. 2010. Differentiating impacts of land use changes from
477 pasture management in a CEAP watershed using the SWAT model. *Trans. ASABE* **53**(5): 1569–1584.

478 Christoffersen BO, Restrepo-Coupe N, Arain MA, Baker IT, Cestaro BP, Ciais P, Fisher JB, Galbraith D,
479 Guan X, Gulden L, others. 2014. Mechanisms of water supply and vegetation demand govern the
480 seasonality and magnitude of evapotranspiration in Amazonia and Cerrado. *Agricultural and Forest*
481 *meteorology* **191**: 33–50. DOI: 10.1016/j.agrformet.2014.02.008.

482 Cleveland WS. 1981. LOWESS: A program for smoothing scatterplots by robust locally weighted
483 regression. *American Statistician* 54–54. DOI: 10.2307/2683591.

484 Climate-Data.org. 2015. *Climate data for cities worldwide*. *http://en.climate-data.org/, Accessed 27*
485 *May 2015*.

486 Coe MT, Costa MH, Soares-Filho BS. 2009. The influence of historical and potential future
487 deforestation on the stream flow of the Amazon River – Land surface processes and atmospheric
488 feedbacks. *Journal of Hydrology* **369**(1–2): 165–174. DOI: 10.1016/j.jhydrol.2009.02.043.

489 Costa MH, Botta A, Cardille JA. 2003. Effects of large-scale changes in land cover on the discharge of
490 the Tocantins River, Southeastern Amazonia. *Journal of Hydrology* **283**(1–4): 206–217. DOI:
491 10.1016/S0022-1694(03)00267-1.

492 D'Almeida C, Vörösmarty CJ, Hurtt GC, Marengo JA, Dingman SL, Keim BD. 2007. The effects of
493 deforestation on the hydrological cycle in Amazonia: a review on scale and resolution. *International*
494 *Journal of Climatology* **27**(5): 633–647. DOI: 10.1002/joc.1475.

495 Davidson EA, de Araújo AC, Artaxo P, Balch JK, Brown IF, C. Bustamante MM, Coe MT, DeFries RS,
496 Keller M, Longo M, Munger JW, Schroeder W, Soares-Filho BS, Souza CM, Wofsy SC. 2012. The
497 Amazon basin in transition. *Nature* **481**(7381): 321–328. DOI: 10.1038/nature10717.

498 De Paiva RCD, Buarque DC, Collischonn W, Bonnet M-P, Frappart F, Calmant S, Bulhões Mendes CA.
499 2013. Large-scale hydrologic and hydrodynamic modeling of the Amazon River basin. *Water*
500 *Resources Research* **49**(3): 1226–1243. DOI: 10.1002/wrcr.20067.

501 De Roo A, Odijk M, Schmuck G, Koster E, Lucieer A. 2001. Assessing the effects of land use changes
502 on floods in the Meuse and Oder catchment. *Physics and Chemistry of the Earth, Part B: Hydrology,*
503 *Oceans and Atmosphere* **26**(7): 593–599.

504 DeFries R, Eshleman KN. 2004. Land-use change and hydrologic processes: a major focus for the
505 future. *Hydrological Processes* **18**(11): 2183–2186. DOI: 10.1002/hyp.5584.

506 Drewry JJ, Cameron KC, Buchan GD. 2008. Pasture yield and soil physical property responses to soil
507 compaction from treading and grazing — a review. *Soil Research* **46**(3): 237–256. DOI:
508 10.1071/SR07125.

509 ESALQ. 2015. *Escola Superior de Agricultura "Luiz de Queiroz." http://www.esalq.usp.br/gerd/*
510 *Accessed 1 June 2015*.

511 Fearnside PM. 2005. Deforestation in Brazilian Amazonia: history, rates, and consequences.
512 *Conservation biology* **19**(3): 680–688. DOI: 10.1111/j.1523-1739.2005.00697.x.

513 Fearnside PM. 2007. Brazil's Cuiabá-Santarém (BR-163) Highway: the environmental cost of paving a
514 soybean corridor through the Amazon. *Environmental management* **39**(5): 601–614.

515 Fuka DR, Walter MT, MacAlister C, Degaetano AT, Steenhuis TS, Easton ZM. 2014. Using the Climate
516 Forecast System Reanalysis as weather input data for watershed models. *Hydrological Processes*
517 **28**(22): 5613–5623. DOI: 10.1002/hyp.10073.

518 Fukunaga DC, Cecílio RA, Zanetti SS, Oliveira LT, Caiado MAC. 2015. Application of the SWAT
519 hydrologic model to a tropical watershed at Brazil. *CATENA* **125**: 206–213. DOI:
520 10.1016/j.catena.2014.10.032.

521 Galford GL, Melillo J, Mustard JF, Cerri CEP, Cerri CC. 2010. The Amazon Frontier of Land-Use Change:
522 Croplands and Consequences for Greenhouse Gas Emissions. *Earth Interactions* **14**(15): 1–24. DOI:
523 10.1175/2010EI327.1.

524 Gassman PW, Reyes MR, Green CH, Arnold JG. 2007. Soil and Water Assessment Tool: Historical
525 Development, Applications, and Future Research Directions, The. *Center for Agricultural and Rural*
526 *Development Iowa State University* **Working Paper 07**-**WP 443**.

527 George C. 2014. Simulation of Hydrologic Impacts of Land Use Land Cover Changes in a Humid
528 Tropical River Basin. .

529 Giambelluca TW, Scholz FG, Bucci SJ, Meinzer FC, Goldstein G, Hoffmann WA, Franco AC, Buchert
530 MP. 2009. Evapotranspiration and energy balance of Brazilian savannas with contrasting tree density.
531 *Agricultural and Forest Meteorology* **149**(8): 1365–1376. DOI: 10.1016/j.agrformet.2009.03.006.

532 Global Weather Data. 2015. *http://globalweather.tamu.edu/ Accessed 31 May 2015*.

533 Göpel J, Schaldach R. this issue. Sustainable land management in Southern Amazonia: Model-based
534 analysis of the robustness of carbon-optimized management systems under global change pressures.
535 .

536 Granier A, Loustau D, Bréda N. 2000. A generic model of forest canopy conductance dependent on
537 climate, soil water availability and leaf area index. *Annals of Forest Science* **57**(8): 11. DOI:
538 10.1051/forest:2000158.

539 Guse B, Pfannerstill M, Fohrer N. 2015. Dynamic modelling of land use change impacts on nitrate
540 loads in rivers. *Environmental Processes* **2**(4): 575–592.

541 Guzha A, Nobrega R, Kovacs K, Amorim RSS, Gerold G. 2013a. Quantifying impacts of agro-industrial
542 expansion in Mato Grosso, Brazil, on watershed hydrology using the Soil and Water Assessment Tool
543 (SWAT) model. paper presented at the Conference: 20th International Congress on Modelling and
544 Simulation. Adelaide, Australia. DOI: 10.5194/hessd-12-9915-2015.

545 Guzha A, Nobrega R, Santos C, Gerold G. 2013b. Investigating discharge and rainfall variability in an
546 Amazonian watershed: Do any trends exist? *IAHS-AISH publication* 346–351.

547 Hayhoe SJ, Neill C, Porder S, Mchorney R, Lefebvre P, Coe MT, Elsenbeer H, Krusche AV. 2011.
548 Conversion to soy on the Amazonian agricultural frontier increases streamflow without affecting
549 stormflow dynamics. *Global Change Biology* **17**(5): 1821–1833. DOI: 10.1111/j.1365-
550 2486.2011.02392.x.

551 Hodnett MG, da Silva LP, da Rocha HR, Cruz Senna R. 1995. Seasonal soil water storage changes
552 beneath central Amazonian rainforest and pasture. *Journal of Hydrology* **170**(1–4): 233–254. DOI:
553 10.1016/0022-1694(94)02672-X.

554 Hunke P, Mueller EN, Schröder B, Zeilhofer P. 2015a. The Brazilian Cerrado: assessment of water and
555 soil degradation in catchments under intensive agricultural use. *Ecohydrology* **8**(6): 1154–1180. DOI:
556 10.1002/eco.1573.

557 Hunke P, Roller R, Zeilhofer P, Schröder B, Mueller EN. 2015b. Soil changes under different land-uses
558 in the Cerrado of Mato Grosso, Brazil. *Geoderma Regional* **4**: 31–43. DOI:
559 10.1016/j.geodrs.2014.12.001.

560 Jacomine PKT. 2013. A nova classificacao brasileira de solos. *Anais da Academia Pernambucana de
561 Ciência Agronômica* **5**(0): 161–179.

562 Kergoat L. 1998. A model for hydrological equilibrium of leaf area index on a global scale. *Journal of
563 Hydrology* **212**–**213**: 268–286. DOI: 10.1016/S0022-1694(98)00211-X.

564 Koch FJ, van Griensven A, Uhlenbrook S, Tekleab S, Teferi E. 2012. The Effects of Land use Change on
565 Hydrological Responses in the Choke Mountain Range (Ethiopia)-A new Approach Addressing Land
566 Use Dynamics in the Model SWAT. *Proceedings of 2012 International Congress on Environmental
567 Modeling and Software Managing Resources of a Limited Planet, Sixth Biennial Meeting, Leipzig,
568 Germany*, 1–5.

569 Lambin EF, Turner BL, Geist HJ, Agbola SB, Angelsen A, Bruce JW, Coomes OT, Dirzo R, Fischer G,
570 Folke C, George PS, Homewood K, Imbernon J, Leemans R, Li X, Moran EF, Mortimore M,
571 Ramakrishnan PS, Richards JF, Skånes H, Steffen W, Stone GD, Svedin U, Veldkamp TA, Vogel C, Xu J.
572 2001. The causes of land-use and land-cover change: moving beyond the myths. *Global
573 Environmental Change* **11**(4): 261–269. DOI: 10.1016/S0959-3780(01)00007-3.

574 Lathuillière MJ, Johnson MS, Donner SD. 2012. Water use by terrestrial ecosystems: temporal
575 variability in rainforest and agricultural contributions to evapotranspiration in Mato Grosso, Brazil.
576 *Environmental Research Letters* **7**(2): 24024. DOI: 10.1088/1748-9326/7/2/024024.

577 Lima LS, Coe MT, Filho BSS, Cuadra SV, Dias LCP, Costa MH, Lima LS, Rodrigues HO. 2013. Feedbacks
578 between deforestation, climate, and hydrology in the Southwestern Amazon: implications for the
579 provision of ecosystem services. *Landscape Ecology* **29**(2): 261–274. DOI: 10.1007/s10980-013-9962-
580 1.

581 Lima W de P, Zakia MB, Libardi PL, de Souza Filho AP, others. 1990. Comparative evapotranspiration
582 of eucalyptus, pine and natural "cerrado" vegetation measure by the soil water balance method".
583 *Ipef International, Piracicaba*.

584 Macedo MN, DeFries RS, Morton DC, Stickler CM, Galford GL, Shimabukuro YE. 2012. Decoupling of
585 deforestation and soy production in the southern Amazon during the late 2000s. *Proceedings of the
586 National Academy of Sciences* **109**(4): 1341–1346. DOI: 10.1073/pnas.1111374109.

587 Macioscheck B. 2013. Land use classification upper Jamanxim catchment. ESRI ArcGIS shape files.
588 Göttingen, Germany.

589 Maia SMF, Ogle SM, Cerri CEP, Cerri CC. 2010. Soil organic carbon stock change due to land use
590 activity along the agricultural frontier of the southwestern Amazon, Brazil, between 1970 and 2002.
591 *Global Change Biology* **16**(10): 2775–2788. DOI: 10.1111/j.1365-2486.2009.02105.x.

592 Mani A, Devi MU, Ramulu V, others. 2014. Simulation of Impact of Change in Landuse on Water Yield
593 of Upper Manair Catchment. *International Journal of Innovative Research and Development* **3**(1).

594 McGrath DA, Smith CK, Gholz HL, Oliveira F de A. 2001. Effects of Land-Use Change on Soil Nutrient
595 Dynamics in Amazônia. *Ecosystems* **4**(7): 625–645. DOI: 10.1007/s10021-001-0033-0.

596 Miles L, Newton AC, DeFries RS, Ravilious C, May I, Blyth S, Kapos V, Gordon JE. 2006. A global
597 overview of the conservation status of tropical dry forests. *Journal of Biogeography* **33**(3): 491–505.
598 DOI: 10.1111/j.1365-2699.2005.01424.x.

599 Mishra SK, Singh VP. 2003. *Soil Conservation Service Curve Number (SCS-CN) Methodology*. Springer
600 Science & Business Media.

601 Moriasi DN, Arnold JG, Van Liew MW, Bingner RL, Harmel RD, Veith TL. 2007. Model evaluation
602 guidelines for systematic quantification of accuracy in watershed simulations. *Trans. Asabe* **50**(3):
603 885–900.

604 Müller H, Rufin P, Griffiths P, Barros Siqueira AJ, Hostert P. 2015. Mining dense Landsat time series
605 for separating cropland and pasture in a heterogeneous Brazilian savanna landscape. *Remote Sensing*
606 *of Environment* **156**: 490–499. DOI: 10.1016/j.rse.2014.10.014.

607 Nandakumar N, Mein RG. 1997. Uncertainty in rainfall—runoff model simulations and the
608 implications for predicting the hydrologic effects of land-use change. *Journal of Hydrology* **192**(1–4):
609 211–232. DOI: 10.1016/S0022-1694(96)03106-X.

610 Negri AJ, Adler RF, Xu L, Surratt J. 2004. The impact of Amazonian deforestation on dry season
611 rainfall. *Journal of Climate* **17**(6): 1306–1319.

612 Nobre CA, Sellers PJ, Shukla J. 1991. Amazonian Deforestation and Regional Climate Change. *Journal*
613 *of Climate* **4**(10): 957–988. DOI: 10.1175/1520-0442(1991)004<0957:ADARCC>2.0.CO;2.

614 Nobrega RLB, A. C. Guzha, G. N. Torres, K. Kovacs, G. Lamparter, R. S. S. Amorim, E. Couto, G. Gerold.
615 2015. Identifying hydrological responses of micro-catchments under contrasting land use in the
616 Brazilian Cerrado. *Hydrology and Earth System Sciences* **19**. DOI: 10.5194/hessd-12-9915-2015.

617 Oliveira PS. 2014. Balanço hídrico e erosão do solo no Cerrado Brasileiro. Sao Paulo, School of
618 engineering, department of hydraulics and sanitary engineering.

619 Oliveira PTS, Nearing MA, Moran MS, Goodrich DC, Wendland E, Gupta HV. 2014. Trends in water
620 balance components across the Brazilian Cerrado. *Water Resources Research* **50**(9): 7100–7114. DOI:
621 10.1002/2013WR015202.

622 Pai N, Saraswat D. 2011. SWAT 2009 _LUC: A Tool to Activate the Land Use Change Module in SWAT
623 2009. *Transactions of the ASABE* **54**(5): 1649–1658.

624 Pongratz J, Bounoua L, DeFries RS, Morton DC, Anderson LO, Mauser W, Klink CA. 2006. The Impact
625 of Land Cover Change on Surface Energy and Water Balance in Mato Grosso, Brazil. *Earth Interactions*
626 **10**(19): 1–17. DOI: 10.1175/EI176.1.

627 Price K. 2011. Effects of watershed topography, soils, land use, and climate on baseflow hydrology in
628 humid regions: A review. *Progress in physical geography* **35**(4): 465–492.

629 Rodrigues ASL, Ewers RM, Parry L, Souza C, Veríssimo A, Balmford A. 2009. Boom-and-Bust
630 Development Patterns Across the Amazon Deforestation Frontier. *Science* **324**(5933): 1435–1437.
631 DOI: 10.1126/science.1174002.

632 Schaldach R, Alcamo J, Koch J, Kölking C, Lapola DM, Schüngel J, Priess JA. 2011. An integrated
633 approach to modelling land-use change on continental and global scales. *Environmental Modelling &*
634 *Software* **26**(8): 1041–1051. DOI: 10.1016/j.envsoft.2011.02.013.

635 Schaldach R, Koch J. 2009. Conceptual design and implementation of a model for the integrated
636 simulation of large-scale land-use systems. In: Athanasiadis DIN, Rizzoli PAE, Mitkas PA and Gómez
637 PD-IJM (eds) *Information Technologies in Environmental Engineering*. Springer Berlin Heidelberg,
638 425–438, DOI:10.1007/978–3–540–88351–7_32.

639 Scheffler R, Neill C, Krusche AV, Elsenbeer H. 2011. Soil hydraulic response to land-use change
640 associated with the recent soybean expansion at the Amazon agricultural frontier. *Agriculture,*
641 *Ecosystems & Environment* **144**(1): 281–289. DOI: 10.1016/j.agee.2011.08.016.

642 Schilling KE, Jha MK, Zhang Y-K, Gassman PW, Wolter CF. 2008. Impact of land use and land cover
643 change on the water balance of a large agricultural watershed: Historical effects and future
644 directions. *Water Resources Research* **44**(7): W00A09. DOI: 10.1029/2007WR006644.

645 Schlicht S. 2013. Dynamics of deforestation and agricultural production in the upper Rio das Mortes
646 watershed in Mato Grosso state (Brazil). M.Sc thesis, Göttingen, Germany, University of Göttingen.

647 Schneider R. 1963. *Groundwater Proviceces Brazil*. Preared in coopertaion with the Government of
648 Brazil and the United Staes Operation Mission to Brazil. Washington, USA.

649 Schönenberg R, Hartberger, Korbinian, Schumann, Charlotte, Guggenberger, Georg, Siebold, Mathias,
650 Boy, Jens, Lakes, Lamparter, Gabriele, Schindewolf, Marcus, Nendel, Claas, Hohnwald, Stefan, Gerold,
651 Gerhard, Klingler, Michael. this issue. Methods of inter- and transdisciplinary research – a trajectory
652 of knowledge integration. .

653 Sellers PJ, Randall D a., Collatz G j., Berry J a., Field C b., Dazlich D a., Zhang C, Collelo G d., Bounoua L.
654 1996. A Revised Land Surface Parameterization (SiB2) for Atmospheric GCMS. Part I: Model
655 Formulation. *Journal of Climate* **9**(4): 676–705. DOI: 10.1175/1520-
656 0442(1996)009<0676:ARLSPF>2.0.CO;2.

657 Sellers PJ, Shuttleworth WJ, Dorman JL, Dalcher A, Roberts JM. 1989. Calibrating the Simple
658 Biosphere Model for Amazonian Tropical Forest Using Field and Remote Sensing Data. Part I: Average
659 Calibration with Field Data. *Journal of Applied Meteorology* **28**(8): 727–759. DOI: 10.1175/1520-
660 0450(1989)028<0727:CTSBMF>2.0.CO;2.

661 Strauch M, Volk M. 2013. SWAT plant growth modification for improved modeling of perennial
662 vegetation in the tropics. *Ecological Modelling* **269**: 98–112. DOI: 10.1016/j.ecolmodel.2013.08.013.

663 usouthal.edu. 2016. *Brzilian Geological Map*. .

664 Wagner PD, Bhallamudi SM, Narasimhan B, Kantakumar LN, Sudheer KP, Kumar S, Schneider K,
665 Fiener P. 2016. Dynamic integration of land use changes in a hydrologic assessment of a rapidly
666 developing Indian catchment. *Science of The Total Environment* **539**: 153–164. DOI:
667 10.1016/j.scitotenv.2015.08.148.

668 Wertz-Kanounnikoff SA. 2005. Forest policy enforcement at the Amazon frontier : the case of Mato
669 Grosso, Brazil. Dissertation.

670 ZEE ZEE. 2015. *, http://www.zee.mg.gov.br/. http://www.zee.mg.gov.br/ Accessed 31 May 2015*.

671

672

673
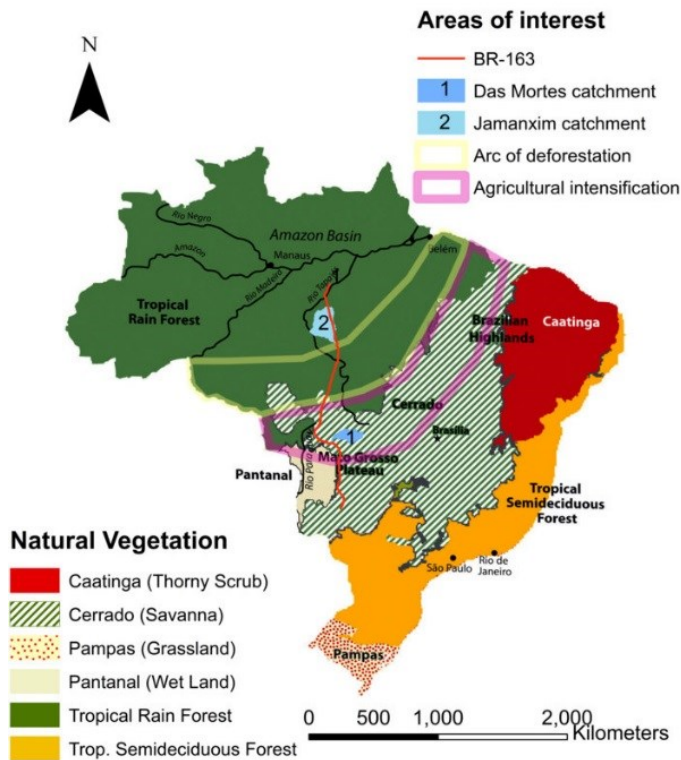
Figure :1 Vegetation biomes in Brazil, locations of the study catchments, the BR-163 and the current
extent of the Amazon agricultural frontier (base map from "Forests in Brazil" 2015; frontier
reproduced after "Global Forest Watch" 2015)

Table 1: Main land use types during the historic calibration and validation period (Landsat imagery
evaluation and *statistical data) and for future LUC scenarios (developed with LANDSHIFT (Göpel and
Schaldach, this issue)

	Das Mortes catchment			Jamanxim catchment		
Historic	**1970**	**1988**	**1998**	**1998**	**2007**	**2011**
Cerrado and Forest	97.5*	64.26	39.79	95.34	91.42	85.03
Cropland	-	-	-	0.10	0.03	0.09
Non-Forest/Pasture	2.00*	35.57	59.89	4.34	8.34	14.57
Trend Scenario	**2020**	**2025**	**2030**	**2020**	**2025**	**2030**
Cerrado and Forest	12.53	11.42	10.96	83.31	79.59	77.20
Cropland	54.31	54.31	54.31	9.91	10.06	10.09
Pasture	32.93	34.04	34.50	5.42	9.17	11.61
Sustainable Scenario	**2020**	**2025**	**2030**	**2020**	**2025**	**2030**
Cerrado and Forest	13.24	12.42	11.66	88.10	88.10	88.10
Cropland	64.29	65.70	67.12	9.90	9.90	10.04
Pasture	22.25	21.65	21.00	0.21	0.21	0.08
Legal Int. Scenario	**2020**	**2025**	**2030**	**2020**	**2025**	**2030**
Cerrado and Forest	14.00	13.61	13.40	82.30	76.67	65.24
Cropland	63.92	64.31	64.48	7.46	12.29	23.71
Pasture	21.86	21.86	21.89	10.04	10.04	10.04
Illegal Int. Scenario	**2020**	**2025**	**2030**	**2020**	**2025**	**2030**
Cerrado and Forest	17.05	16.66	16.39	69.94	66.82	64.56
Cropland	60.58	60.97	61.23	18.14	21.20	23.46
Pasture	22.15	22.14	22.16	11.04	11.14	11.17

Table 2: Optimum calibration parameter values for land use dependent top soil parameters

Land use	Das Mortes					Jamanxim		
	Gallery forest	Non-Forest Pasture	Non-Forest Cropland	Cerrado			Rain-forest	Pasture
CN	44	58	48	35			36	60
k_{sat} Latosolo vermelho mm h^{-1}	183		117	262	k_{sat} Argilosolo mm h^{-1}		461	453
k_{sat} Latosolo Vermelho amarelo mm h^{-1}	559		407	594	k_{sat} Latosolo vermelho-amarelo mm h^{-1}		670	587
k_{sat} Neosolo mm h^{-1}	103	120		224	k_{sat} Neosolo mm h^{-1}		221	212

Table 3: Calibration Statistics for the Model calibration, validation and steady land use application in both study catchments for a monthly time step calibration (coefficient of determination: R², Nash-Sutcliffe Efficiency index: NS, percentual bias: PBIAS, p- and r-factor of the 95% confidence interval)

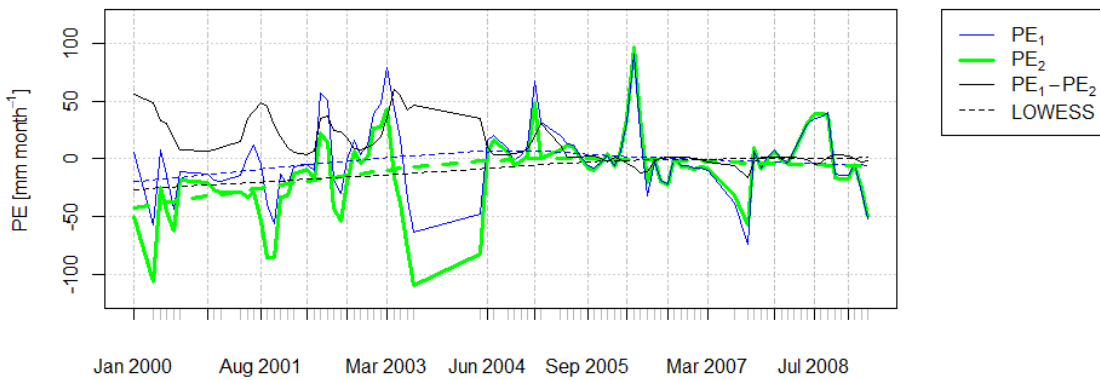|	Das Mortes					Jamanxim				
	R²	NS	PBIAS	p-factor	r-factor	R²	NS	PBIAS	p-factor	r-factor
Calibration	0.85	0.74	-4.54	0.84	0.87	0.8	0.8	-0.5	0.60	0.47
Validation	0.79	0.73	-8.1	0.91	0.86	0.8	0.8	0.8	0.42	0.63
steady land use	0.84	0.61	-16.4	0.81	0.99	0.8	0.8	1.7	0.52	0.48

Prediction errors das Mortes catchment
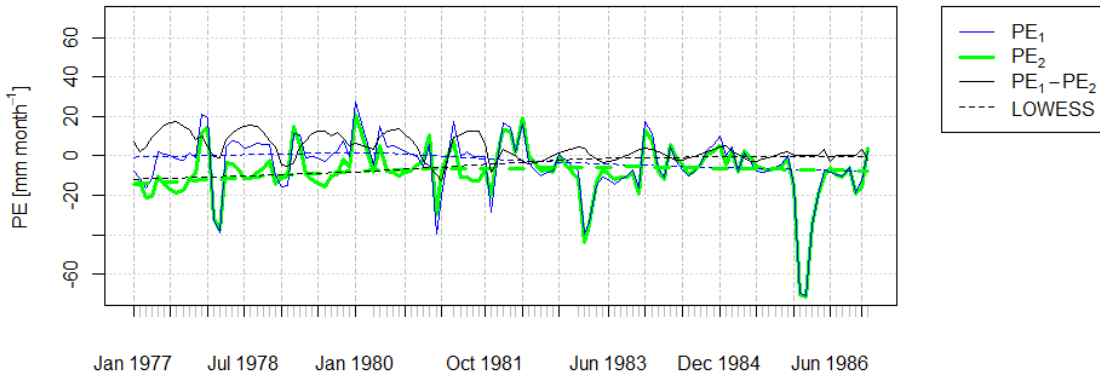
687

**Prediction errors Jamanxim catchment**

688

689 *Figure 2a Das Mortes catchment model, Prediction Error*
690 *(PE=Qobs-Qmod) of the land use update (PE$_1$) and steady*
691 *land use (PE$_2$) setup, difference in PE (PE$_1$-PE$_2$) and LOWESS*
692 *trend lines of all latter, for the calibration and validation*

693 *2b Jamanxim catchment model, Prediction Error (PE=Qobs-*
694 *Qmod) of the land use update (PE$_1$) and steady land use (PE$_2$)*
695 *setup, difference in PE (PE$_1$-PE$_2$) and LOWESS trend lines of all*
696 *latter, for the calibration and validation*
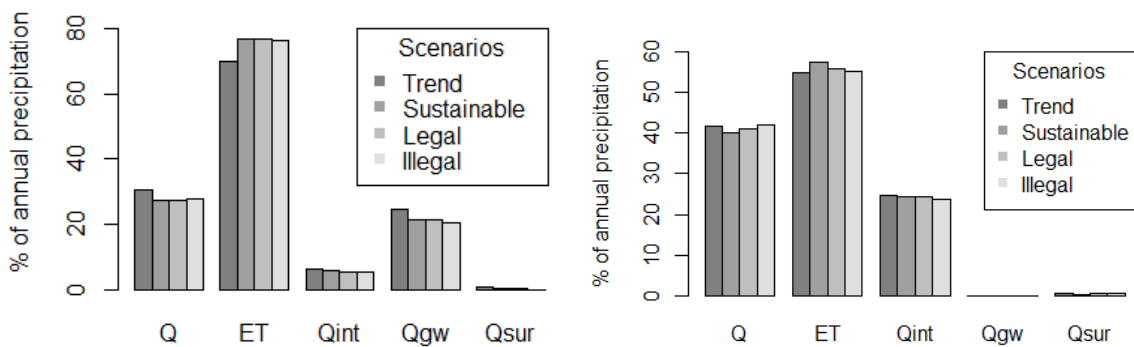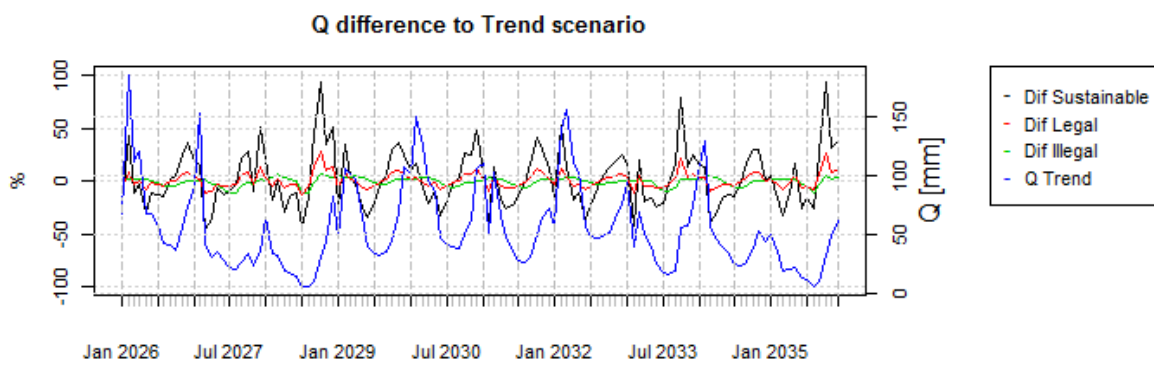

697
698

699 *Figure 3 a and b*

700 *Das Mortes catchment; annual water balance components in relation to mean annual rainfall for model scenario period*
701 *2026 to 2035, Q: discharge, ET: Evapotranspiration, Qint: interflow from shallow aquifer, Qgw: Groundwater or Baseflow*
702 *contribution to discharge, Qsur: Surface runoff contribution to discharge*

706
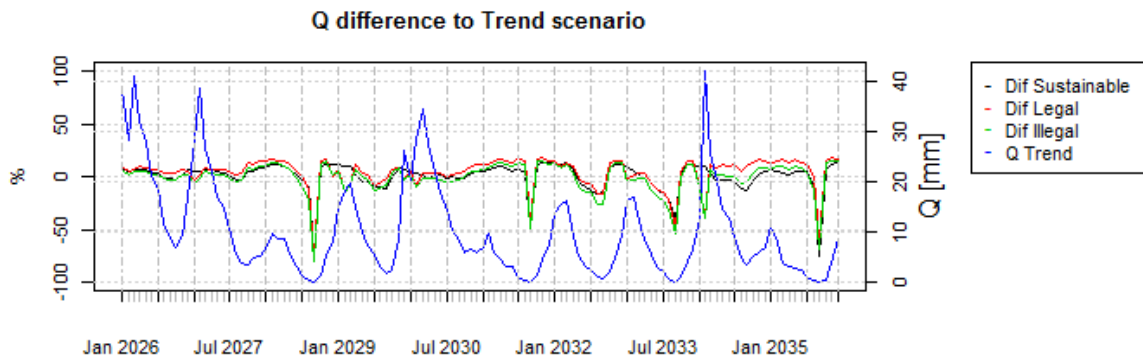
707

708
709 *Figure 4 a: Difference in scenario predicted stream discharge: ΔQ=Qtrend-Qother scenarios, and*
710 *simulated stream discharge for trend scenario, das Mortes catchment*

711 *Figure 5 b: Difference in scenario predicted stream discharge: ΔQ=Qtrend-Qother scenarios, and*
712 *simulated stream discharge for trend scenario, Jamanxim catchment*

713

714
715

716